Supplementary Information

Multilayer Interfacial Engineering of Al–Ce Metallic Glass for Brittleness Mitigation and Reliable Motion Sensing

Jae Sang Cho[a,+], Emad S. Goda[b,+], Woongsik Jang[b,c], Keum Hwan Park[d], Dong Hwan Wang[a,b,*]

[a]Department of Intelligent Semiconductor Engineering, Chung-Ang University, 84 Heukseok-ro, Dongjak-gu, Seoul 06974, Republic of Korea

[b]School of Integrative Engineering, Chung-Ang University, 84 Heukseok-ro, Dongjak-gu, Seoul 06974, Republic of Korea

[c]Center for Polymers and Organic Solids and Department of Chemistry and Biochemistry, University of California at Santa Barbara Santa Barbara, CA 93106, USA

[d]Display Research Center Korea Electronics Technology Institute 25 Saenari-ro, Bundang-gu, Seongnam-si, Gyeonggi-do, 13509, Republic of Korea

†These authors contributed equally to this work.

* Corresponding author, E-mail king0401@cau.ac.kr (Prof. D.H. Wang)

Keywords: Metallic glass, nanoindentation, shear banding, strain sensor, motion sensing

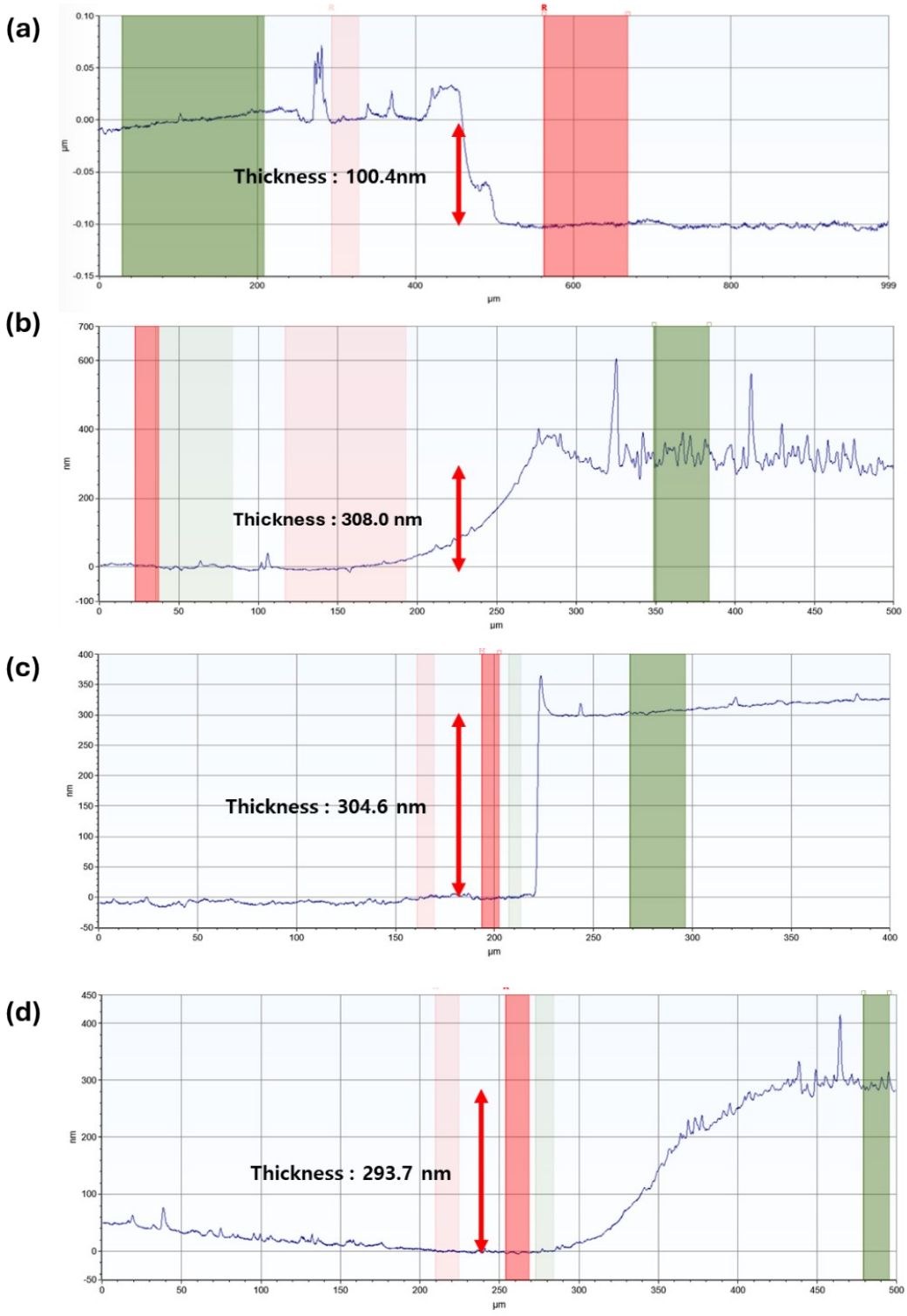

Fig. S1. Thickness measurements of (a) 100 nm amorphous AlCe, (b) 300 nm crystalline Al, (c) 300 nm amorphous AlCe, and (d) 300 nm multilayered metallic glass using an alpha-step surface profiler.

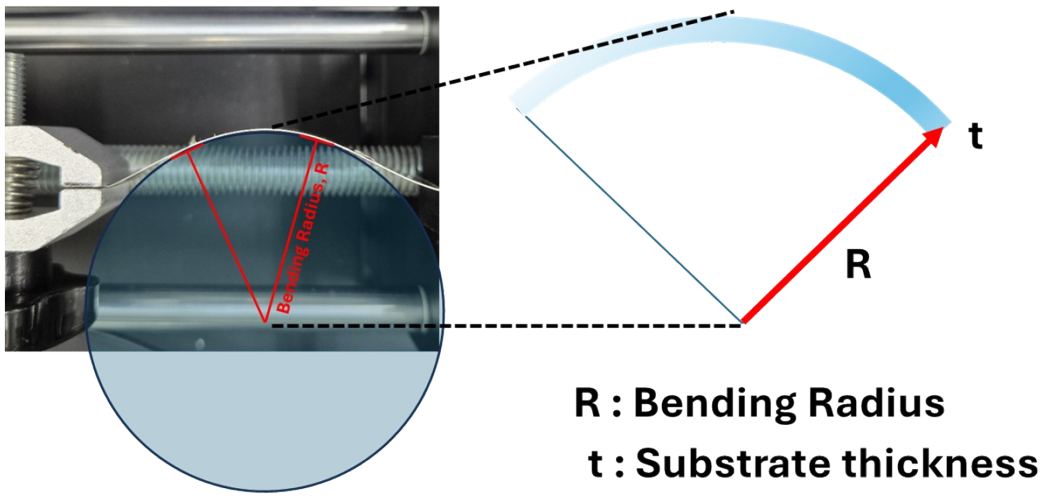

Fig. S2. Photograph of the bending test setup and a schematic illustration of the parameters used for bending strain calculation.

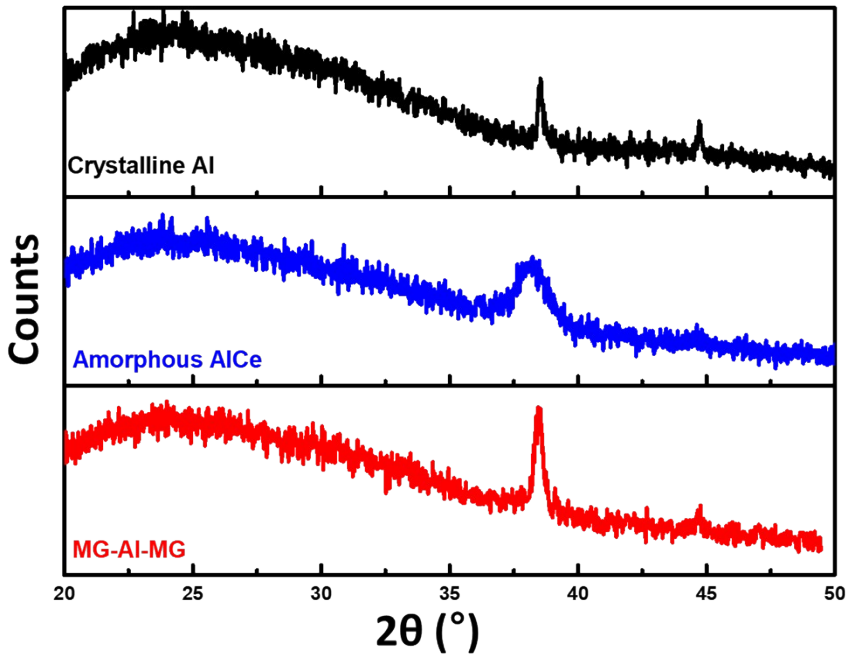

Fig. S3. X-ray diffraction profiles of crystalline Al, amorphous AlCe, and the multilayered metallic glass.

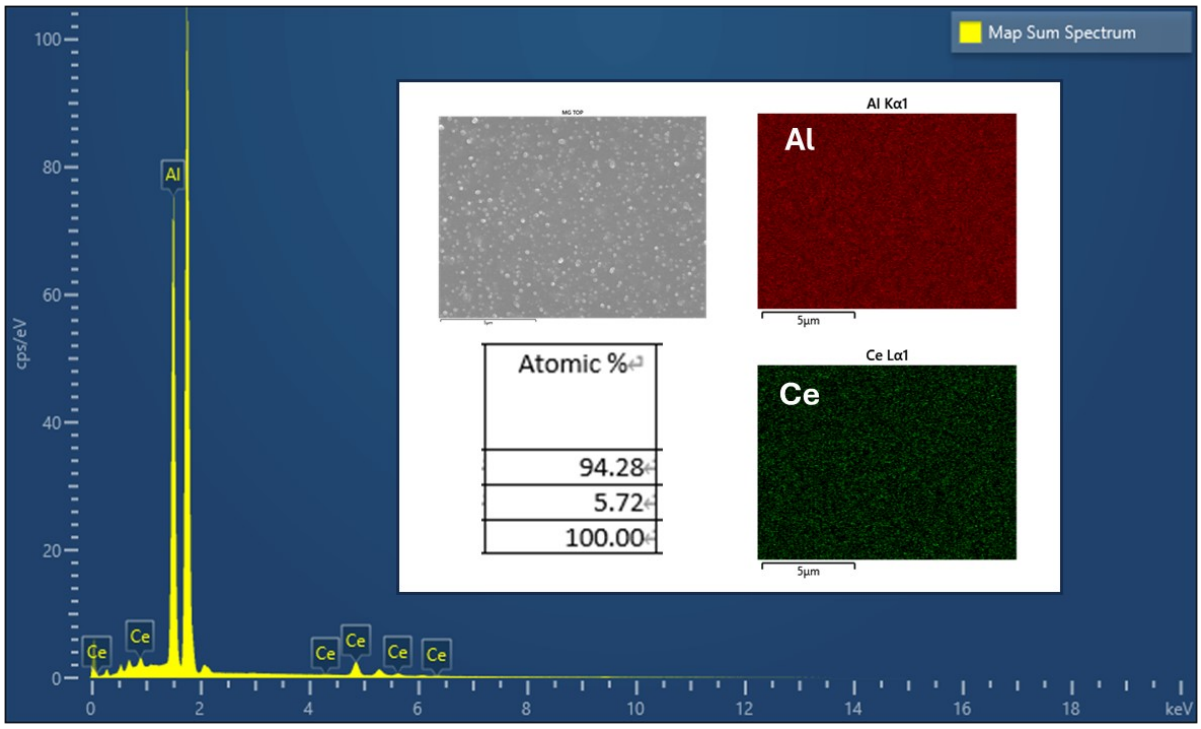

Fig. S4. Compositional analysis of the sputtered amorphous AlCe layer, showing the atomic ratio of Al and Ce.

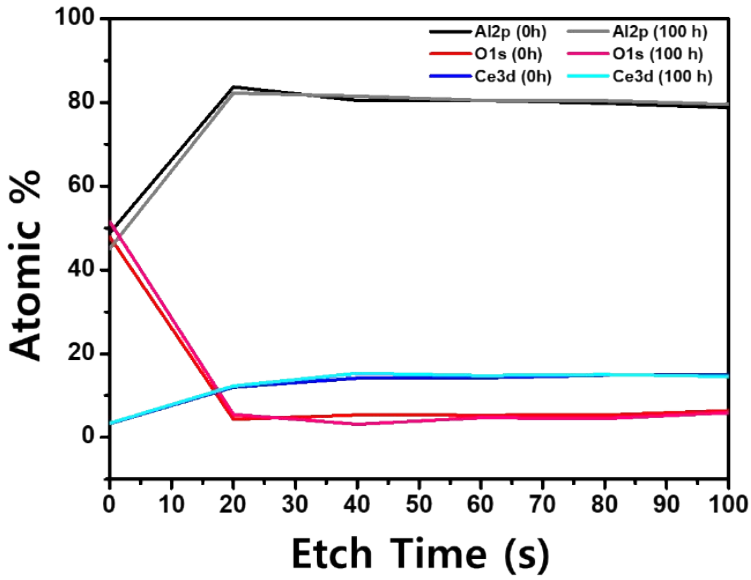

Fig. S5. XPS depth profile of AlCe metallic glass electrode, demonstrating the absence of internal oxygen contamination and the pristine metallic state of the interfaces.

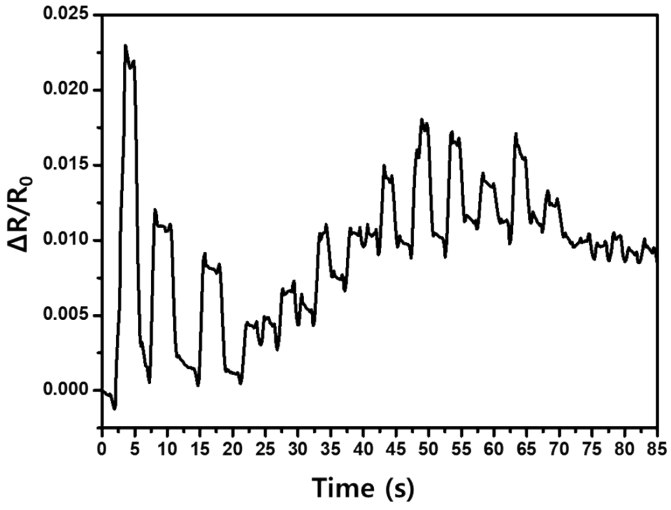

Fig. S6. Results of the cyclic bending test under a bending strain of 0.8% obtained from crystalline Al thin film.

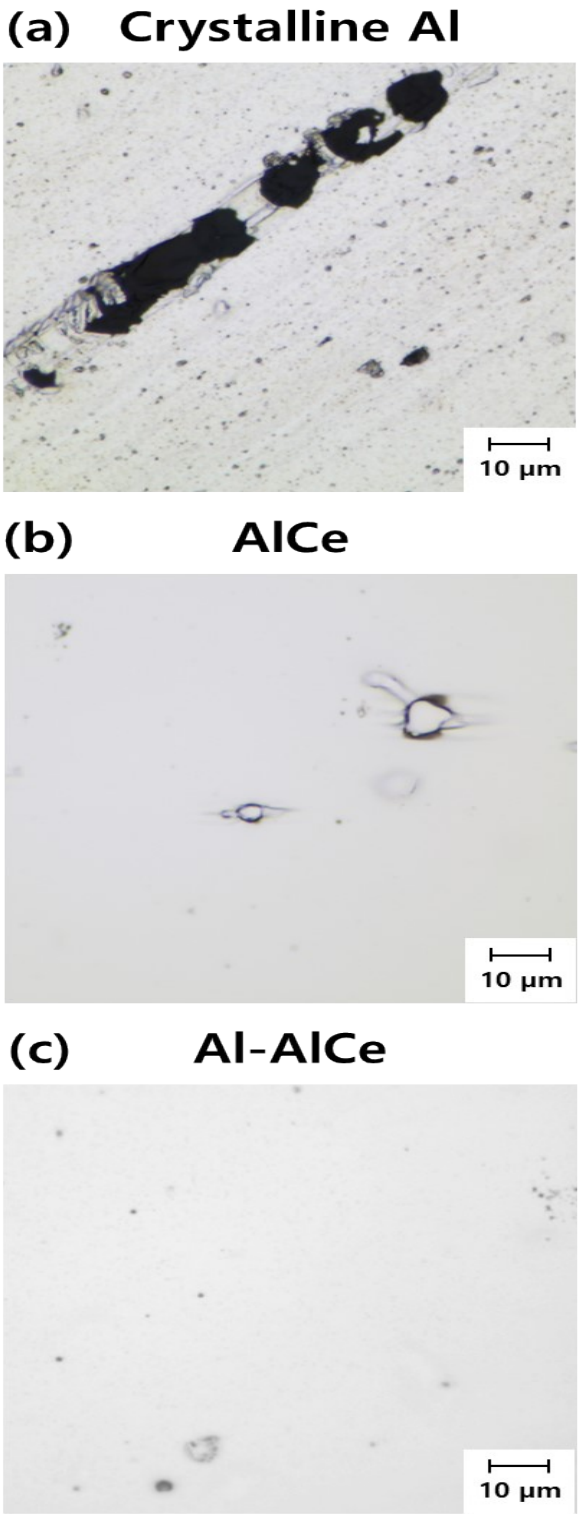

Fig. S7. Optical microscopy (OM) images of the electrode surfaces after the severe bending test. (a) Single-layer crystalline Al exhibiting catastrophic crack propagation and severe delamination. (b) Single-layer amorphous AlCe showing localized shear bands evolving into micro-cracks. (c) The pristine, entirely crack-free surface of the AlCe metallic glass layer deposited on Al layer (Al-AlCe).

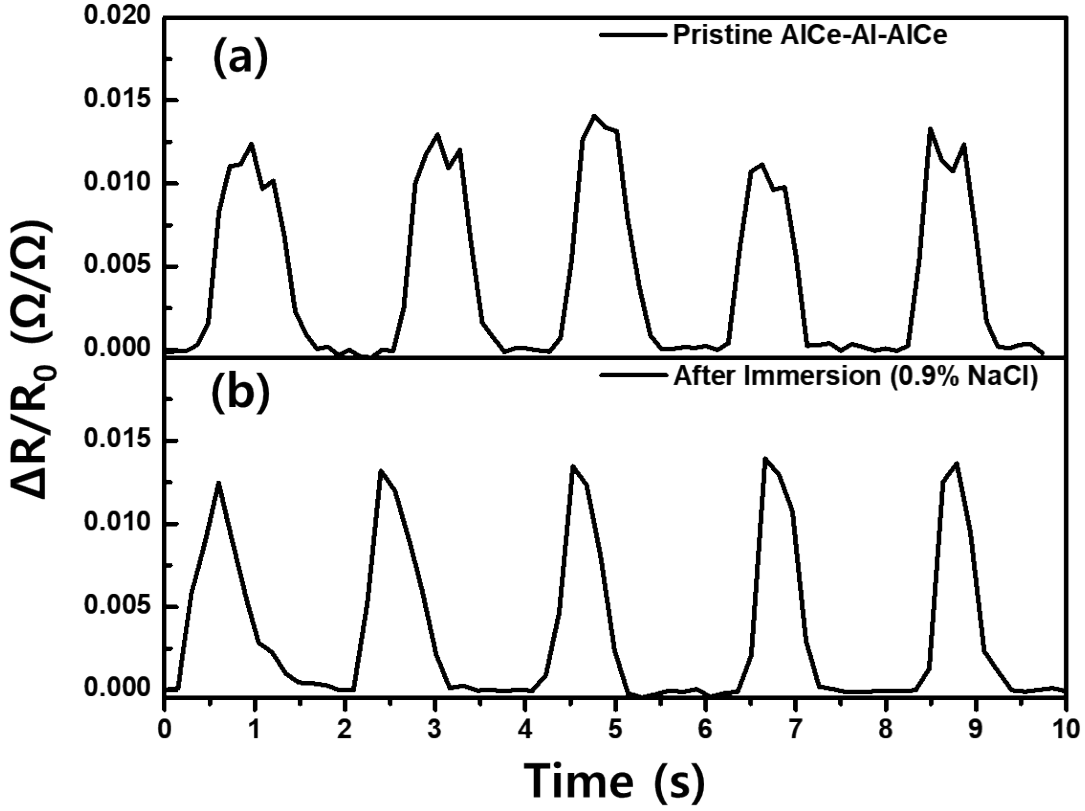

Fig. S8. Evaluation of the piezoresistive stability in a simulated sweaty environment. Strain-sensing responses of the multilayer electrode (a) before and (b) after complete immersion in a 0.9% NaCl saline solution for 100 minutes.

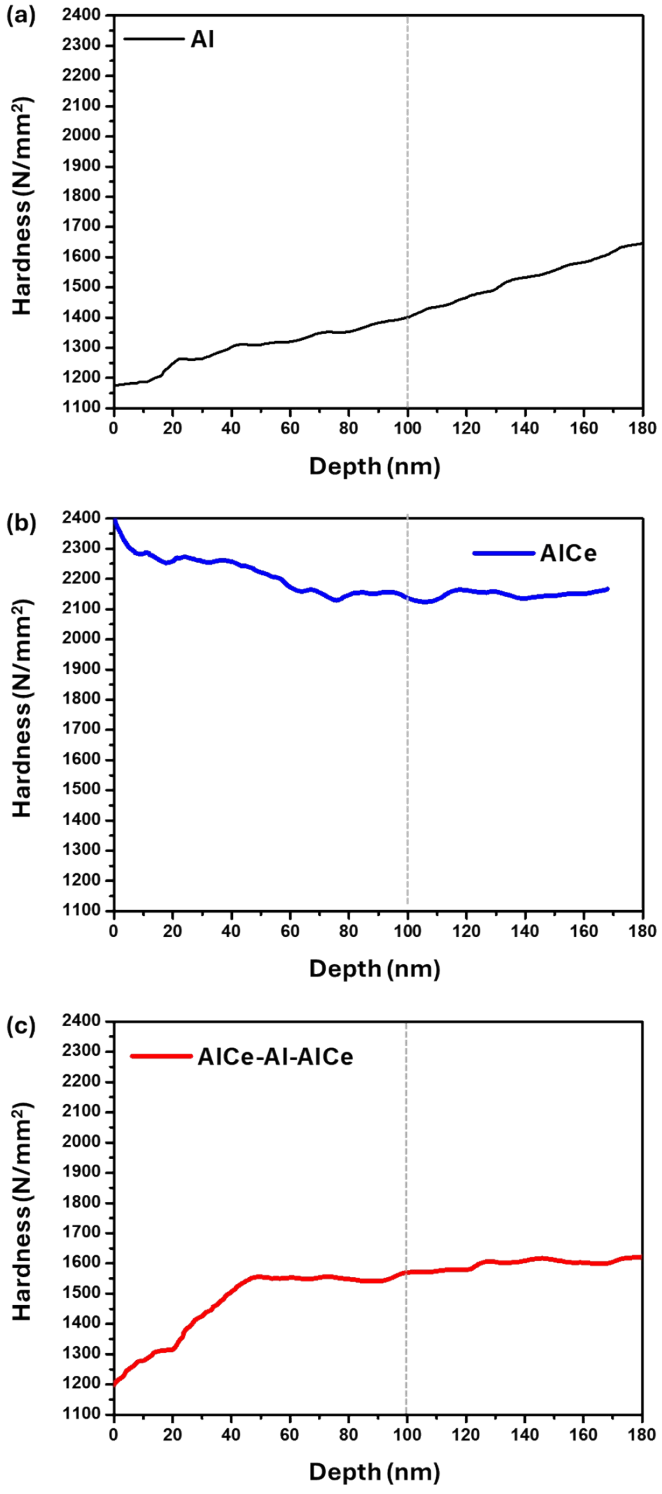

Fig. S9. Vickers hardness measurements according to the indentation depth, (a) crystalline Al, (b) amorphous AlCe, (c) multilayered AlCe-Al-AlCe

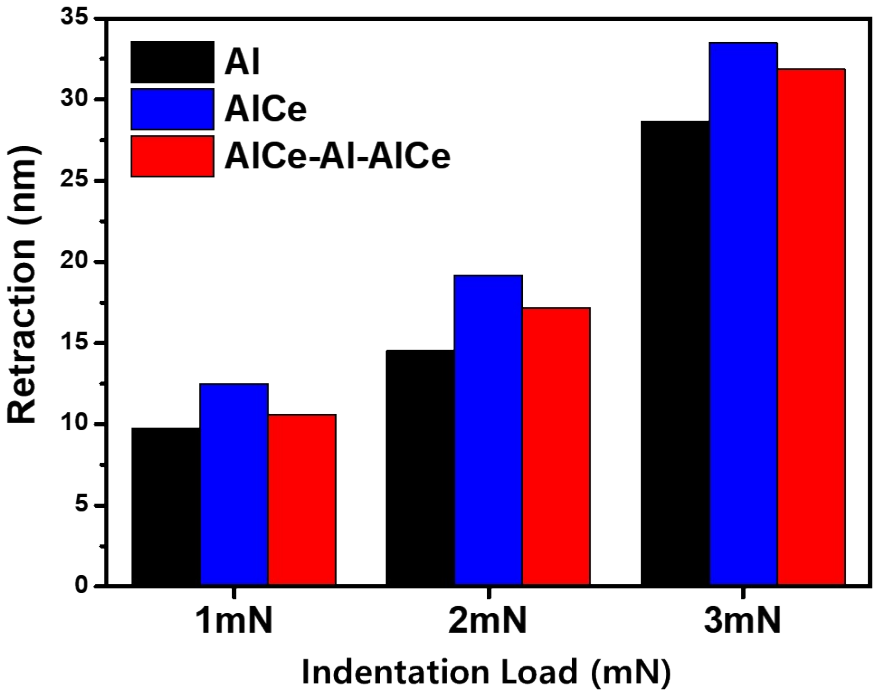

Fig. S10. Retraction distances from nanoindentation analyses of Al, AlCe, and multilayered metallic glass under varying indentation loads.

Table S1. Full width at half maximum (FWHM) of the X-ray diffraction peak at $2\theta = 38.51°$ for the investigated electrodes.

Electrode	FWHM
Crystalline Al	0.228
Amorphous AlCe	1.109
Multilayer MG	0.370

Table S2. Comparison of strain sensing performances of MG-based electrodes in previously reported studies.

Composition	Electrode Type	Thickness/Diameter (nm)	Gauge Factor	Maximum Strain (%)	Linearity (R^2)	Ref
$Pd_{40}Cu_{30}Ni_{10}P_{20}$	Fiber	70000	2.28	2.20	0.99	[S1]
$Pd_{40}Cu_{30}Ni_{10}P_{20}$	Fiber	6500	2.22	2.16	0.99	[S2]
$Zr_{55}Cu_{30}Ni_5Al_{10}$	Thin Film	300	2.86	1.00	0.99	[S3]
$Zr_{58}Al_{14}Ni_{11}Co_{16}$	Thin Film	100	1.1	0.70	0.98	[S4]
$Zr_{55}Cu_{30}Al_{10}Ni_5$	Thin Film	110	1.1~4.3	0.19	N.A.	[S5]
$Al_{94}Ce_6/Al/Al_{94}Ce_6$	Thin Film	300	3.11	1.10	0.99	This Work

References

[S1] J. Yi, H.Y. Bai, D.Q. Zhao, M.X. Pan, W.H. Wang, Piezoresistance effect of metallic glassy fibers, Appl Phys Lett 98 (2011).

[S2] J. Yi, L. Huo, D. Zhao, M. Pan, H. Bai, W. Wang, Toward an ideal electrical resistance strain gauge using a bare and single straight strand metallic glassy fiber, Sci China Phys Mech Astron 55 (2012) 609–613.

[S3] H.J. Xian, C.R. Cao, J.A. Shi, X.S. Zhu, Y.C. Hu, Y.F. Huang, S. Meng, L. Gu, Y.H. Liu, H.Y. Bai, Flexible strain sensors with high performance based on metallic glass thin film, Appl Phys Lett 111 (2017).

[S4] J.S. Cho, W. Jang, K.H. Park, D.H. Wang, Metallic amorphous alloy for long-term stable electrodes in organic sensors and photovoltaics, Org Electron 84 (2020) 105811.

[S5] Y.-C. Chuang, T.-Y. Cheng, Y.-C. Tsai, Flexible printed circuit board strain sensor embedded in a miniaturized pneumatic finger, IEEE Sens J 22 (2022) 22456–22463.